2015 IEEE 54th Annual Conference on Decision and Control (CDC)
December 15-18, 2015. Osaka, Japan

Fundamental Dynamics based Adaptive Energy Control for Cooperative Swinging of Complex Pendulum-like Objects*

Philine Donner[1,2], Franz Christange[1] and Martin Buss[1,2]

Abstract— **We present an adaptive energy-based controller for cooperative swinging of complex pendulum-like objects by two agents. The complex pendulum-like object has two oscillation degrees of freedom of which one is to be controlled to a goal energy and the other one has to be damped. The closed-loop fundamental dynamics of a simple pendulum are extended to the two-agent pendulum. Based on the fundamental dynamics, a simple adaptive mechanism identifies the natural frequency of the system. An amplitude factor is adapted such that an agent behaves as a leader or a follower. A leader knows the goal energy and controls the system according to desired reference dynamics. A follower either imitates the leader's energy flow or estimates the leader's goal energy. Properties as stability of both leader-follower structures are analyzed analytically based on the fundamental dynamics assumption. The applicability of the control approaches to a complex pendulum-like object is shown in simulation.**

I. INTRODUCTION

Cooperative dynamic manipulation enlarges the manipulation capabilities of multi-agent teams. While *cooperative manipulation* allows for manipulation of heavy and bulky objects that cannot be manipulated by one agent alone, *dynamic manipulation* furthermore exploits the full object dynamics [1]. Driven by this motivation, we discussed model-based approaches for cooperative swinging of complex pendulum-like objects in [2], [3]. The goal of the cooperative swinging task is the excitation of the pendulum-like object such that it stabilizes at a desired energy state. In order to be able to handle unknown objects, adaptive control approaches are needed. In this work, we present an adaptive energy controller for cooperative swinging of complex pendulum-like objects as displayed in Fig. 1.

Pendulum-like objects are also referred to as suspended or slung loads. Within the area of suspended-load transport, e.g. through cranes or quadrotors, the focus has mostly been on damping of oscillations. However, dynamic swing motion can extend workspace and manipulation capabilities. For instance, in [4] a quadrotor injects energy into its suspended load such that it can fly through a vertically limited opening. In the literature, most oscillation exciting controllers originated from the inverted pendulum task, where a pendulum is first swung-up and subsequently stabilized in its unstable equilibrium point, e.g. [5], [6]. Our previous as well as the present work build upon the energy-based swing-up controller by Yoshida [7].

Cooperative dynamic manipulation of pendulum-like objects has hardly been considered. Existing approaches for cooperative suspended load manipulation either focus on oscillation damping [8], [9] or use one centralized controller [10]. In [11] and [12] a robot helps a human with sustaining a rope turning motion. However, the rope turning motion had to be established by the human partner beforehand.

Besides reinforcement learning approaches, only little work can be found on adaptive swing-up controllers. The reinforcement learning community has used inverted pendulum tasks as a benchmark to investigate how well their approaches can control nonlinear systems [13], [14]. The aggressive window passing maneuver of [4] is accomplished through sampling based reinforcement learning initialized by a model-based optimal control solution. In [15], reinforcement learning combined with the model based energy control [7] was applied to the cooperative swinging task discussed in our previous work from a model based perspective [2], [3]. Motivated by the drawback of a high number of tuning parameters [16], [15], we recently presented a simple pendulum adaptive swing-up controller [17]. This adaptive controller is based on the closed loop fundamental dynamics and requires only two tuning parameters: a time constant for the estimation of the natural frequency and a control gain that specifies desired reference dynamics. In this work we extend the fundamental dynamics approach of [17] to two-agent pendulums. We further take a step beyond the leader controller presented in [15] and additionally design two adaptive follower controllers.

The remainder of this paper is structured as follows. Section II formally states the problem. In Sec. III, we derive the fundamental dynamics for a simplified two agent pendulum. Based on the fundamental dynamics, a leader and two follower controllers are designed and analytically analyzed in Sec. IV. In Sec. V, we extend the approach to control a complex pendulum-like object. The applicability of the fundamental dynamics based controller design to the complex pendulum-like object is examined in Sec. VI. Section VII concludes the paper.

II. PROBLEM FORMULATION

A. The t-pendulum

As an example for a complex pendulum-like object we use the two-agent pendulum displayed in Fig. 1. We refer to this

*The research leading to these results has received funding partly from the European Research Council under the European Unions Seventh Framework Programme (FP/2007-2013) / ERC Grant Agreement n. [267877] and partly from the Technische Universität München - Institute for Advanced Study (www.tum-ias.de), funded by the German Excellence Initiative

[1]Chair of Automatic Control Engineering, Technische Universität München, Theresienstr. 90, 80333 München, Germany, {philine.donner, franz.christange, mb}@tum.de

[2]TUM Institute for Advanced Study, Technische Universität München, Lichtenbergstrasse 2a, 85748 Garching, Germany

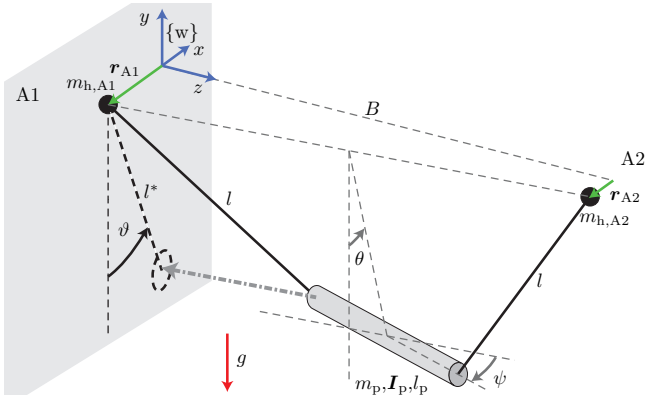

Fig. 1. The t-pendulum: a cylindrical object of mass m_p, length l_p and inertia $\boldsymbol{I}_\mathrm{p}$ suspended through massless ropes of length l from two handles of mass $m_{\mathrm{h},Ai}$ at locations $\boldsymbol{r}_{Ai}$ with $i = 1, 2$. The minimum distance between the two agents is B. The location $\boldsymbol{r}_{A1}$ is defined with respect to the world fixed coordinate system $\{\mathrm{w}\}$. The location $\boldsymbol{r}_{A2}$ is defined with respect to the fixed point ${}^{\mathrm{w}}p = [0 \quad 0 \quad B]^T$ in $\{\mathrm{w}\}$.

pendulum as a t-pendulum because of its trapezoidal shape. We classify the t-pendulum to be a complex pendulum-like object, because it does not only have one oscillation degree of freedom (DoF), but two predominant oscillation DoFs, which are described by the deflection angles θ and ψ. The pendulum is actuated by two agents A1 and A2 through handles located at $\boldsymbol{r}_{A1}$ and $\boldsymbol{r}_{A2}$, respectively.

B. Problem statement for adaptive energy control for cooperative swinging

The overall goal is to control the θ-oscillation to reach the constant energy level E_θ^d, while the ψ-oscillation is regarded as undesired and needs to be damped, i.e. $E_\psi^\mathrm{d} = 0$. The goal energies of the θ- and the ψ-oscillation can equivalently be expressed as desired maximum deflection angles θ_E^d and ψ_E^d. In order for the controller to be model-independent, we replace the mass and inertia dependent energies E_θ and E_ψ with the maximum deflection angles and formulate our control goal as $\theta_E = \theta_E^\mathrm{d}$ and $\psi_E = 0$.

The agents influence the t-pendulum through acceleration of their handles $\ddot{\boldsymbol{r}}_{Ai}$, $i = 1, 2$. For simplicity, we limit the agents to move along the x-axis, i.e. $\boldsymbol{r}_{Ai} = [r_{Ai} \quad 0 \quad 0]^T$. Hence, the state of the t-pendulum is given by $\boldsymbol{x}_\mathrm{t,c} = \begin{bmatrix}\theta & \psi & \dot\theta & \dot\psi & r_{A1} & \dot r_{A1} & r_{A2} & \dot r_{A2}\end{bmatrix}^T$. We further assume that the only feedback the agents receive about the state of the object and the partner's intention are the forces measured at the own interaction point, i.e. for agent A1 $\boldsymbol{y}_\mathrm{m} = \boldsymbol{F}_{A1}$. We assume cooperation between the agents. However, from the perspective of agent A1, the only input is $u = \ddot r_{A1}$, while the acceleration of the partner's handle $z = \ddot r_{A2}$ is a disturbance, as it cannot be directly controlled.

The agents can act as a leader $\mathcal{L}$ or a follower $\mathcal{F}$ (e.g. A1 $= \mathcal{F}$ and A2 $= \mathcal{L}$). A **leader** knows the goal energy of the θ-oscillation θ_E^d. We are looking for a control law

$$\begin{aligned} u_\mathcal{L} = \ddot r_\mathcal{L} &= f(\boldsymbol{F}_\mathcal{L}) \\ \text{such that} \quad &\left|\theta_{E\mathrm{m}} - \theta_E\right| \le \epsilon_\theta \\ \text{with} \quad &\dot\theta_{E\mathrm{m}} = K_\mathrm{d}(\theta_E^\mathrm{d} - \theta_{E\mathrm{m}}), \\ \text{and } &\left|0 - \psi_E(t > T_\mathrm{s})\right| \le \epsilon_\psi, \text{ for } 0 < T_\mathrm{s} < \infty, \end{aligned} \tag{1}$$

where ϵ_θ defines bounds within which the energy of the θ-oscillation is required to follow the first-order reference dynamics $\theta_{E\mathrm{m}}$ of inverse time constant K_d and ϵ_ψ defines bounds within which the energy of the ψ-oscillation is to be kept the latest after the settling time T_s. We limit the goal energy to $\theta_E^\mathrm{d} < \pi/2$, in order to be able to approximate the suspension ropes as rigid.

A **follower** does not know the goal energy of the θ-oscillation θ_E^d. Thus, the follower needs to infer the leader's intention from the measured interaction forces in order to actively contribute to the task goal. We formulate the follower control goal as

$$\begin{aligned} u_\mathcal{F} = \ddot r_\mathcal{F} &= f(\boldsymbol{F}_\mathcal{F}) \\ \text{such that} \quad &\left|\gamma_\mathcal{F}^\mathrm{d} - \gamma_\mathcal{F}\right| \le \epsilon_\mathcal{F} \\ \text{with} \quad &\gamma_\mathcal{F} = \frac{\int_0^{T_\mathrm{s}} \dot\theta_{E,\mathcal{F}}\,\mathrm{d}\tau}{\int_0^{T_\mathrm{s}} \dot\theta_{E,\mathcal{F}} + \dot\theta_{E,\mathcal{L}}\,\mathrm{d}\tau}, \\ \text{and } &\left|0 - \psi_E(t > T_\mathrm{s})\right| \le \epsilon_\psi, \text{ for } 0 < T_\mathrm{s} < \infty, \end{aligned} \tag{2}$$

where $\gamma_\mathcal{F}$ is the relative energy contribution of the follower, which is computed based on the integrals over the energy flows of the leader and the follower $\dot\theta_{E,\mathcal{F}/\mathcal{L}}$. Thus, we want the follower to have contributed the fraction $\gamma_\mathcal{F}^\mathrm{d}$ within bounds $\epsilon_\mathcal{F}$ of the energy effort required to reach the goal energy θ_E^d at the settling time T_s, while also damping the undesired oscillation ψ. The desired relative energy contribution of the follower has to obey $\gamma_\mathcal{F}^\mathrm{d} \in [0,\ 1[$, while the exact value is a design parameter.

III. FUNDAMENTAL DYNAMICS APPLIED TO THE TWO-AGENT PENDULUM

In this section, we apply the fundamental dynamics derived in [17] to the abstract simple pendulum. The abstract simple pendulum is a simple pendulum with two-sided actuation and captures essentials of the desired system behavior. Subsection III-A introduces the abstract simple pendulum and Subsec. III-B the main idea of the the energy-based controller. The two-agent fundamental dynamics are derived in Subsec. III-C.

A. The abstract simple pendulum

The control goal formulated in the previous section ideally results in an oscillation with $\psi = 0$ and $\theta \approx \vartheta$, where ϑ describes the deflection of the t-pendulum when being projected onto the xy-plane of agent A1 (see grey shaded area in Fig. 1). We approximate the desired oscillation seen by agent A1 for the reduced state $\boldsymbol{x}_\mathrm{c} = \begin{bmatrix}\vartheta & \dot\vartheta\end{bmatrix}^T$ as

$$\dot{\boldsymbol{x}}_\mathrm{c} = \begin{pmatrix}\dot\vartheta \\ -\omega_{0,\vartheta}^2 \sin\vartheta\end{pmatrix} + \begin{pmatrix}0 \\ -\frac{1}{g}\omega_{0,\vartheta}^2 \cos\vartheta\end{pmatrix} \frac{\ddot r_{A1} + \ddot r_{A2}}{2}, \tag{3}$$

with gravity g, the small angle approximation of the natural frequency $\omega_{0,\vartheta} = \sqrt{\frac{g}{l^*}}$ and projected length[1] l^* (see Fig. 1). These dynamics represent a simple pendulum with two-sided actuation, which we call the abstract simple pendulum [3].

[1]The projected length l^* changes with r_{Ai} and consequently the natural frequency changes as well. Since the natural frequency is estimated online, our control approach can capture these effects.

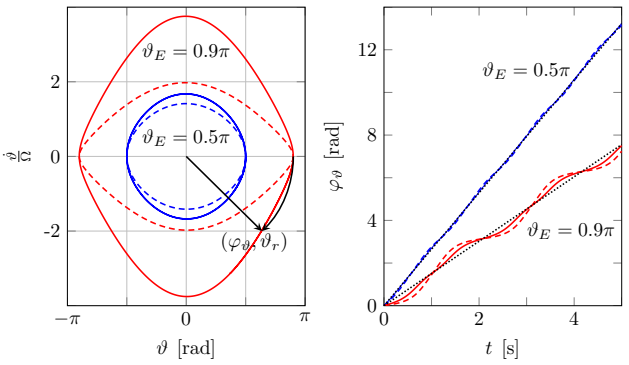

Fig. 2. Phase portrait for a lossless simple pendulum (left) and the resulting phase angle φ over time (right) for two different energy levels ϑ_E. Solid lines indicate normalization with $\Omega = \omega$, dashed lines $\Omega = \omega_{0,\vartheta}$.

The energy contained in the abstract simple pendulum for zero handle velocities is

$$E_\vartheta := E|_{\dot{r}_{\mathrm{A}i}=0} = \frac{1}{2} m_\mathrm{p} (l^*)^2 \dot{\vartheta}^2 + m_\mathrm{p} g l^* \left(1 - \cos\vartheta\right). \quad (4)$$

The energy E_ϑ can equivalently be expressed by the amplitude ϑ_E. The amplitude ϑ_E is equal to the maximum deflection angle ϑ, which is reached at the turning points

$$E_\vartheta = m_\mathrm{p} g l^* \left(1 - \cos\vartheta_E\right). \quad (5)$$

Insertion of (4) into (5) and solving for the energy equivalent ϑ_E yields

$$\vartheta_E = \arccos\left(\cos\vartheta - \frac{l^*}{2g}\dot{\vartheta}^2\right), \quad (6)$$

with $\vartheta_E \in [0,\ \pi]$. Due to the independence of the parameter pendulum mass m_p, we use ϑ_E instead of E_ϑ to refer to the system energy throughout the rest of the paper.

Simple pendulums are highly nonlinear systems. The system nonlinearities become apparent in the energy dependent natural frequency $\omega_\vartheta(\vartheta_E)$. No analytic solution exists for the natural frequency, but it can be calculated numerically by the arithmetic-geometric mean [18]. The nonlinear nature of simple pendulums is also visible in its phase space. This is illustrated for two different energy levels $\vartheta_E = \{0.5\pi, 0.9\pi\}$ at the left hand side of Fig. 2. The highlighted phase angle is calculated as

$$\varphi_\vartheta = \mathrm{atan2}\left(-\frac{\dot{\vartheta}}{\Omega}, \vartheta\right), \quad (7)$$

where the variable Ω is a normalization factor. The phase angle describes the oscillation state of the pendulum, e.g. $\varphi_\vartheta = \frac{\pi}{2}$ when the pendulum crosses the lower equilibrium from $\vartheta > 0$ to $\vartheta < 0$. The right hand side of Fig. 2 shows the phase angle over time. The closer the normalization factor Ω is to the real natural frequency ω_ϑ, the more circle-like is the phase portrait and the more linearly rises the phase angle over time

$$\varphi_\vartheta(t) \approx \omega_\vartheta t + \varphi_\vartheta(t = 0), \quad (8)$$

with $\varphi_\vartheta(t = 0) = 0$ in Fig. 2. Consequently, the simple pendulum system appears to be linear for small energies and normalization with $\Omega = \omega_\vartheta$. For small energies, the small angle approximation $\omega_{0,\vartheta}$ can serve as a good estimate for the actual natural frequency ω_ϑ. For high energies, the nonlinearities become more apparent, especially when only the small angle approximation is used for normalization $\Omega = \omega_{0,\vartheta}$ (see right side of Fig. 2).

B. Energy based swing-up control

The energy control is based on the swing-up control of [7]. The complete control law is given in Sec. V. The following derivations are based on the approximate control law

$$\ddot{r}_{\mathrm{A}i} \approx a_{\mathrm{A}i}\, \omega_\vartheta^2 \sin\varphi_\vartheta, \quad (9)$$

which captures the main idea of the swing-up controller. The multiplication with $\sin\varphi_\vartheta$ excites the pendulum at its natural frequency ω_ϑ according to (8). The amplitude factor $a_{\mathrm{A}i}$ specifies direction and amount of energy flow to the pendulum. The derivation of the amplitude factor $a_{\mathrm{A}i}$ is explained in Sec. IV-B.

C. Fundamental dynamics for the abstract simple pendulum

The following is based on the fundamental dynamics derivation given in [17]. Insertion of the approximate control law (9) into the abstract simple pendulum dynamics (3) results in a highly nonlinear system with states $\boldsymbol{x}_\mathrm{c} = \begin{bmatrix}\vartheta & \dot{\vartheta}\end{bmatrix}^T$, which clearly depend on each other. A coordinate transformation to phase angle φ_ϑ and system energy ϑ_E would ideally decouple the states[2], because the system energy ϑ_E does not depend on the phase angle φ_ϑ. However, solving (7) for $\dot{\vartheta}$ and insertion of $\dot{\vartheta}$ into (6) yields

$$\cos\vartheta_E = \cos\vartheta - \frac{\Omega^2}{2\omega_{0,\vartheta}^2} \tan^2(\varphi_\vartheta)\, \vartheta^2, \quad (10)$$

for which we cannot find an analytic expression $\vartheta(\varphi_\vartheta, \vartheta_E)$. For this reason, we use the phase space radius ϑ_r

$$\vartheta_r := \sqrt{\vartheta^2 + \left(\frac{\dot{\vartheta}}{\Omega}\right)^2}, \quad (11)$$

which approximates the system energy ϑ_E (see Fig. 2) and form the polar coordinates $\boldsymbol{x}_\mathrm{p} = \begin{bmatrix}\varphi_\vartheta & \vartheta_r\end{bmatrix}^T$.

The following steps are applied to derive the fundamental dynamics. For details see [17]. First, we differentiate (7) and (11) with respect to time. In a second step, we insert the abstract simple pendulum dynamics and substitute all cartesian states with polar states according to

$$\begin{aligned} \vartheta &= \vartheta_r \cos\varphi_\vartheta \\ \dot{\vartheta} &= -\vartheta_r \Omega \sin\varphi_\vartheta. \end{aligned} \quad (12)$$

In a third step, we insert the approximate control law (9) and the normalization factor $\Omega = \omega_\vartheta$. Finally, we simplify the system of equations through approximation with 3rd order Taylor polynomials, negligence of higher harmonics

[2]Note that this decoupling is only valid for a slowly changing natural frequency $\omega_\vartheta \approx$ const., such that the phase φ_ϑ is independent of the system energy ϑ_E.

and usage of the geometric mean as an approximation for the natural frequency $\omega_\vartheta \approx \omega_{0,\vartheta}\sqrt{\cos\frac{\vartheta_r}{2}}$ for $\vartheta_r \approx \vartheta_E$. The result are the fundamental dynamics of the closed-loop abstract simple pendulum of the form

$$\dot{\boldsymbol{x}}_\mathrm{p} = \begin{pmatrix}\dot{\varphi}_\vartheta \\ \dot{\vartheta}_r\end{pmatrix} = \begin{pmatrix}\omega_\vartheta \\ 0\end{pmatrix} + \begin{pmatrix}0 \\ B\end{pmatrix}\frac{a_{\mathrm{A}1}+a_{\mathrm{A}2}}{2}$$
$$\text{with } B = \frac{1}{2g}\omega_\vartheta^3 = \text{const.}, \tag{13}$$

which we use in the following section to design an adaptive energy controller that estimates the natural frequency ω_ϑ and designs decentralized control inputs $a_{\mathrm{A}i}$, $i = 1, 2$. The fundamental dynamics are treated as if they are decoupled and $\omega_\vartheta = \text{const.}$. In reality, however, the frequency depends on the energy content $\omega_\vartheta(\vartheta_r)$. We implicitly take the energy dependence into account because we online adapt to the changing frequency of the system ω_ϑ [17].

IV. ADAPTIVE ENERGY CONTROL BASED ON THE FUNDAMENTAL DYNAMICS

The fundamental dynamics show how the system energy $\vartheta_E \approx \vartheta_r$ will change dependent on the choice of the amplitude factor $a_{\mathrm{A}1/\mathrm{A}2}$ in control law (9) and an estimate of the natural frequency $\hat{\omega}_\vartheta$. In this section, we first present the $\hat{\omega}_\vartheta$-adaptation (Subsec. IV-A). This is followed by the leader and follower dependent computation of the amplitude factor $a_{\mathrm{A}i}$ in Subsec. IV-B. In Subsec. IV-C, we analyze properties as stability of the proposed leader-follower structures. Let us for now assume full state feedback $\boldsymbol{x}_\mathrm{c} = \begin{bmatrix}\vartheta & \dot{\vartheta}\end{bmatrix}^T$ from which the polar state $\boldsymbol{x}_\mathrm{p} = [\varphi_\vartheta \quad \vartheta_r]^T$ can be computed based on an estimate of the natural frequency $\hat{\omega}_\vartheta$.

A. Adaptation of natural frequency estimate $\hat{\omega}_\vartheta$

The same simple adaptation mechanism for the natural frequency estimate is used as in [17]

$$\hat{\omega}_\vartheta = \frac{s}{1+T_\omega s}\varphi_\vartheta, \tag{14}$$

with T_ω being a time constant that defines the speed of the adaptation. A Lyapunov based stability analysis is given in [17]. It shows under the fundamental dynamics assumption that the adaptation converges to the exact natural frequency as long as the conservative constraint $T_\omega > \frac{1}{2\hat{\omega}_\vartheta}$ is fulfilled.

B. Computation of amplitude factor $a_{\mathrm{A}i}$

While the leader and the follower use the same $\hat{\omega}_\vartheta$-adaptation for the computation of the phase φ_ϑ as needed for the control law (9), they differ in the way they determine the amplitude factor $a_{\mathrm{A}i}$.

1) Leader $\mathcal{L}$: The **leader** knows the desired energy $\vartheta_r^\mathrm{d} = \theta_r^\mathrm{d} \approx \theta_E^\mathrm{d}$ (see (1)). Similar to [7], we apply the saturated mapping from energy error $\theta_E^\mathrm{d} - \vartheta_r$ to amplitude factor $a_\mathcal{L}$

$$a_\mathcal{L} = \begin{cases} \bar{a}\,\mathrm{sgn}(\theta_E^\mathrm{d} - \vartheta_r) & \text{if } k_\mathcal{L}|\theta_E^\mathrm{d} - \vartheta_r| \geq \bar{a} \\ k_\mathcal{L}(\theta_E^\mathrm{d} - \vartheta_r) & \text{else,}\end{cases} \tag{15}$$

with control gain $k_\mathcal{L} > 0$, which defines the slope of the mapping that is saturated at a maximum amplitude factor $\pm\bar{a}$. In this case, the leader injects energy into the pendulum $a_\mathcal{L} > 0 \rightarrow \dot{\vartheta}_{r,\mathcal{L}} > 0$ as long as the system energy is below the desired energy $\theta_E^\mathrm{d} - \vartheta_r > 0$, but withdraws energy from the pendulum $a_\mathcal{L} < 0 \rightarrow \dot{\vartheta}_{r,\mathcal{L}} < 0$ in case the system energy exceeds the desired energy $\theta_E^\mathrm{d} - \vartheta_r < 0$, with $\dot{\vartheta}_{r,\mathcal{L}}$ being the energy flow produced by the leader (see (13)).

As defined in (1), the total system energy is supposed to follow first-order reference dynamics during swing-up

$$\dot{\theta}_{E\mathrm{m}} \quad = \quad K_\mathrm{d}\left(\theta_E^\mathrm{d} - \theta_{E\mathrm{m}}\right). \tag{16}$$

Let $\gamma_\mathcal{L}^\mathrm{d} \in]0, 1]$ define the relative contribution of the leader, equivalently as defined for the follower in (2). The desired relative contribution is achieved if $\dot{\vartheta}_{\mathcal{L},r} \stackrel{!}{=} \gamma_\mathcal{L}^\mathrm{d}\dot{\vartheta}_r$ at all times. Solving this relationship for $\dot{\vartheta}_r$ and insertion of the fundamental dynamics $\dot{\vartheta}_{\mathcal{L},r} = \frac{B}{2}a_\mathcal{L}$ (see (13)) and the linear part of the proportional controller of (15) yields

$$\dot{\vartheta}_r \quad = \quad \frac{1}{\gamma_\mathcal{L}^\mathrm{d}}\frac{B}{2}k_\mathcal{L}\left(\theta_E^\mathrm{d} - \vartheta_r\right). \tag{17}$$

From (16) and (17) we deduce $K_\mathrm{d} \stackrel{!}{=} \frac{1}{\gamma_\mathcal{L}^\mathrm{d}}\frac{B}{2}k_\mathcal{L}$, such that ideally $\theta_{E\mathrm{m}}{=}\vartheta_r$ and the control gain results in

$$k_\mathcal{L} = \frac{2\gamma_\mathcal{L}^\mathrm{d}K_\mathrm{d}}{\hat{B}} \tag{18}$$

with estimate $\hat{B}(\hat{\omega}_\vartheta)$ according to the fundamental dynamics in (13). Note that the controller saturates if tracking of the first-order reference dynamics requires an amplitude $a_\mathcal{F}$ that exceeds the amplitude limits $\pm\bar{a}$ (see (15)).

2) Follower $\mathcal{F}$: The **follower** has to contribute with a relative contribution $\gamma_\mathcal{F}^\mathrm{d} \in [0, 1[$ to the overall task effort without knowledge of the desired energy θ_E^d (see (2)). This demanded relative contribution is achieved if $\dot{\vartheta}_{\mathcal{F},r} \stackrel{!}{=} \gamma_\mathcal{F}^\mathrm{d}\dot{\vartheta}_r$ at all times. Based on this requirement we present two follower approaches in the following.

The **flow imitation** approach achieves $\dot{\vartheta}_{\mathcal{F},r} = \gamma_\mathcal{F}^\mathrm{d}\dot{\vartheta}_r$ by a saturated mapping from estimated total energy flow to the pendulum $\hat{\dot{\vartheta}}_r$ to amplitude factor $a_\mathcal{F}$ under consideration of the fundamental dynamics in (13)

$$a_\mathcal{F} = \begin{cases} \bar{a}\,\mathrm{sgn}(\hat{\dot{\vartheta}}_r) & \text{if } |\tfrac{2}{\hat{B}}\gamma_\mathcal{F}^\mathrm{d}\hat{\dot{\vartheta}}_r| \geq \bar{a} \\ \frac{2}{\hat{B}}\gamma_\mathcal{F}^\mathrm{d}\hat{\dot{\vartheta}}_r & \text{else.}\end{cases} \tag{19}$$

We obtain the total energy flow estimate through filtered differentiation $\hat{\dot{\vartheta}}_r = G_\mathrm{hp}\vartheta_r$, where $G_\mathrm{hp}(T_f)$ is a first-order high-pass filter[3] with time constant T_f.

The **goal estimation** approach assumes that the leader's energy flow is determined by the linear reference dynamics (16) with gain $\hat{K}_\mathrm{d}$ and a desired relative energy contribution $\hat{\gamma}_\mathcal{L}^\mathrm{d} = 1 - \gamma_\mathcal{F}^\mathrm{d}$. Together with an estimate of the leader's energy flow $\hat{\dot{\vartheta}}_{r,\mathcal{L}} = G_\mathrm{hp}(T_f)\vartheta_r - G_\mathrm{lp}(T_f)\hat{\dot{\vartheta}}_{r,\mathcal{F}}$ with $\hat{\dot{\vartheta}}_{r,\mathcal{F}} = \frac{\hat{B}}{2}a_\mathcal{F}$ this allows for the estimation of the goal energy

$$\hat{\theta}_E^\mathrm{d} = G_\mathrm{lp}(T_f)\vartheta_r + \frac{1}{\hat{K}_\mathrm{d}(1-\gamma_\mathcal{F}^\mathrm{d})}\hat{\dot{\vartheta}}_{r,\mathcal{L}}. \tag{20}$$

[3]The first-order high-pass filter differentiates ϑ_r up to a frequency of $\omega_\mathrm{c} = \frac{1}{T_f}$, while higher frequency parts of ϑ_r are not altered.

Note that we apply the first-order low-pass filter $G_{\mathrm{lp}}(T_f)$ to obtain the same phase and amplitude shift with respect to the necessary high-pass filtering of the energy equivalent ϑ_r. Based on the estimated goal energy $\hat{\theta}_E^{\mathrm{d}}$, the same mapping of energy error to amplitude factor $a_{\mathcal{F}}$ is applied as for the leader (15), but with control gain

$$k_{\mathcal{F}} = k_\gamma \frac{2\gamma_{\mathcal{F}}^{\mathrm{d}} \hat{K}_{\mathrm{d}}}{\hat{B}}, \tag{21}$$

where the factor k_γ enforces the desired follower contribution $\gamma_{\mathcal{F}}^{\mathrm{d}}$ as described in the following section.

C. Analysis of leader-follower structures

We analyze properties as stability, stationary transfer behavior and resultant follower contribution $\gamma_{\mathcal{F}}^{\mathrm{d}}$ based on the fundamental dynamics and under the assumption that the saturations of the mappings (15) and (19) are not active[4] (for details see [19]). In order to take estimation errors into account, we differentiate between the actual system constant B and the leader and follower estimates $\hat{B}_{\mathcal{L}}$ and $\hat{B}_{\mathcal{F}}$.

The reference input transfer function $\vartheta_r(s) = G^{\mathrm{fi}}(s)\theta_E^{\mathrm{d}}(s)$ of a leader interacting with a **flow imitation** follower is

$$G^{\mathrm{fi}} = \frac{\gamma_{\mathcal{L}}^{\mathrm{d}} K_{\mathrm{d}} \frac{B}{\hat{B}_{\mathcal{L}}} s + \gamma_{\mathcal{L}}^{\mathrm{d}} K_{\mathrm{d}} \frac{B}{\hat{B}_{\mathcal{L}}} \frac{1}{T_f}}{s^2 + (\frac{1}{T_f} - \gamma_{\mathcal{F}}^{\mathrm{d}} \frac{B}{\hat{B}_{\mathcal{F}}} \frac{1}{T_f} + \gamma_{\mathcal{L}}^{\mathrm{d}} K_{\mathrm{d}} \frac{B}{\hat{B}_{\mathcal{L}}}) s + \gamma_{\mathcal{L}}^{\mathrm{d}} K_{\mathrm{d}} \frac{B}{\hat{B}_{\mathcal{L}}} \frac{1}{T_f}} \tag{22}$$

which shows that the stationary transfer behavior is equal to one, i.e. $\vartheta_r(t \to \infty) = \theta_E^{\mathrm{d}}$ for a step of height θ_E^{d} in the reference variable $\theta_E^{\mathrm{d}}(t) = \sigma(t)\theta_E^{\mathrm{d}}$. Note that this holds independent of estimation errors ($\hat{B}_{\mathcal{F}/\mathcal{L}} \neq B$ when $\hat{\omega}_\vartheta \neq \omega_\vartheta$ in (13)).

The closed loop system is asymptotically stable for $(\frac{1}{T_f} - \gamma_{\mathcal{F}}^{\mathrm{d}} \frac{B}{\hat{B}_{\mathcal{F}}} \frac{1}{T_f} + \gamma_{\mathcal{L}}^{\mathrm{d}} K_{\mathrm{d}} \frac{B}{\hat{B}_{\mathcal{L}}}) > 0$. The stability constraints imply that the follower's $\hat{\omega}_\vartheta$-adaptation should be initialized high enough ($\hat{B}_{\mathcal{F}} > B$) and that estimation errors together with a high desired follower contribution $\gamma_{\mathcal{F}}^{\mathrm{d}}$ and small time constant T_f can potentially lead to instability.

The final value theorem applied to the follower transfer function $\vartheta_{r,\mathcal{F}}(s) = G_{\mathcal{F}}^{\mathrm{fi}}(s)\theta_E^{\mathrm{d}}(s)$ yields $\vartheta_{r,\mathcal{F}}(t \to \infty) = \gamma_{\mathcal{F}}^{\mathrm{d}} \frac{B}{\hat{B}_{\mathcal{F}}} \theta_E^{\mathrm{d}}$. Consequently, the follower achieves its desired relative contribution for a correct $\hat{\omega}_\vartheta$ estimate ($B = \hat{B}_{\mathcal{F}}$).

The reference input transfer function $\vartheta_r(s) = G^{\mathrm{ge}}(s)\theta_E^{\mathrm{d}}(s)$ of a leader interacting with a **goal estimation** follower is

$$G^{\mathrm{ge}} = \frac{\gamma_{\mathcal{L}}^{\mathrm{d}} K_{\mathrm{d}} \frac{B}{\hat{B}_{\mathcal{L}}} s + \gamma_{\mathcal{L}}^{\mathrm{d}} K_{\mathrm{d}} \frac{B}{\hat{B}_{\mathcal{L}}} \frac{1}{T_f} (1 + k_\gamma \frac{\gamma_{\mathcal{F}}^{\mathrm{d}}}{1-\gamma_{\mathcal{F}}^{\mathrm{d}}})}{\begin{aligned} s^2 + (&\frac{1}{T_f} + \frac{k_\gamma}{T_f} \frac{\gamma_{\mathcal{F}}^{\mathrm{d}}}{1-\gamma_{\mathcal{F}}^{\mathrm{d}}} (1 - \frac{B}{\hat{B}_{\mathcal{F}}}) + k_\gamma \gamma_{\mathcal{F}}^{\mathrm{d}} \hat{K}_{\mathrm{d}} \frac{B}{\hat{B}_{\mathcal{F}}} + \\ &+ \gamma_{\mathcal{L}}^{\mathrm{d}} K_{\mathrm{d}} \frac{B}{\hat{B}_{\mathcal{L}}}) s + \gamma_{\mathcal{L}}^{\mathrm{d}} K_{\mathrm{d}} \frac{B}{\hat{B}_{\mathcal{L}}} \frac{1}{T_f} (1 + k_\gamma \frac{\gamma_{\mathcal{F}}^{\mathrm{d}}}{1-\gamma_{\mathcal{F}}^{\mathrm{d}}}) \end{aligned}} \tag{23}$$

and consequently exhibits a stationary transfer behavior of one $\vartheta_r(t \to \infty) = \theta_E^{\mathrm{d}}$ similar to the flow imitation approach.

[4]According to simulations, saturations did not affect the stationary transfer behavior with respect to ϑ_r and $\hat{\theta}_E^{\mathrm{d}}$, but did alter the follower contribution $\gamma_{\mathcal{F}}$. The stability borders were the same. However, the saturated system did not become unstable but only marginally stable.

The follower contribution based on the final value theorem $\vartheta_{r,\mathcal{F}}(t \to \infty) = \gamma_{\mathcal{F}} \theta_E^{\mathrm{d}}$ is

$$\gamma_{\mathcal{F}} = \frac{1 + k_\gamma \frac{\gamma_{\mathcal{F}}^{\mathrm{d}}}{1-\gamma_{\mathcal{F}}^{\mathrm{d}}} - k_\gamma \gamma_{\mathcal{F}}^{\mathrm{d}} \frac{B}{\hat{B}_{\mathcal{F}}} (\frac{1}{1-\gamma_{\mathcal{F}}^{\mathrm{d}}} - T_f \hat{K}_{\mathrm{d}})}{1 + k_\gamma \frac{\gamma_{\mathcal{F}}^{\mathrm{d}}}{1-\gamma_{\mathcal{F}}^{\mathrm{d}}}}. \tag{24}$$

We compute the gain k_γ such that the desired follower contribution is enforced as long as the $\hat{\omega}_\vartheta$ estimate is correct $\vartheta_{r,\mathcal{F}}(t \to \infty, B = \hat{B}_{\mathcal{F}}) \stackrel{!}{=} \gamma_{\mathcal{F}}^{\mathrm{d}} \theta_E^{\mathrm{d}}$ which yields

$$k_\gamma = \frac{1}{1 - T_f \hat{K}_{\mathrm{d}}}. \tag{25}$$

If we limit the gain k_γ to reasonable values $k_\gamma > 0$, the goal estimation approach is asymptotically stable for $(\frac{1}{T_f} + \frac{k_\gamma}{T_f} \frac{\gamma_{\mathcal{F}}^{\mathrm{d}}}{1-\gamma_{\mathcal{F}}^{\mathrm{d}}} (1 - \frac{B}{\hat{B}_{\mathcal{F}}}) + k_\gamma \gamma_{\mathcal{F}}^{\mathrm{d}} \hat{K}_{\mathrm{d}} \frac{B}{\hat{B}_{\mathcal{F}}} + \gamma_{\mathcal{L}}^{\mathrm{d}} K_{\mathrm{d}} \frac{B}{\hat{B}_{\mathcal{L}}}) > 0$ (see (23)). Consequently, similar guidelines apply as for the flow imitation approach: the absolute stability margin increases with a high initialization of $\hat{B}_{\mathcal{F}}$ and a low desired follower contribution $\gamma_{\mathcal{F}}^{\mathrm{d}}$. The time constant T_f should obey $0 < T_f < \frac{1}{\hat{K}_{\mathrm{d}}}$.

A further question that arises for the goal estimation approach is whether the follower identifies the goal energy correctly. The transfer function from goal energy θ_E^{d} to estimated goal energy $\hat{\theta}_E^{\mathrm{d}}$ is $G_{\hat{\theta}_E^{\mathrm{d}}}^{\mathrm{ge}} = G_{\vartheta_r \to \hat{\theta}_E^{\mathrm{d}}}^{\mathrm{ge}} G^{\mathrm{ge}}$ with

$$G_{\vartheta_r \to \hat{\theta}_E^{\mathrm{d}}}^{\mathrm{ge}} = \frac{\frac{1}{\hat{K}_{\mathrm{d}}(1-\gamma_{\mathcal{F}}^{\mathrm{d}})} s + k_\gamma \frac{\gamma_{\mathcal{F}}^{\mathrm{d}}}{1-\gamma_{\mathcal{F}}^{\mathrm{d}}} + 1}{T_f s + k_\gamma \frac{\gamma_{\mathcal{F}}^{\mathrm{d}}}{1-\gamma_{\mathcal{F}}^{\mathrm{d}}} + 1}. \tag{26}$$

Hence, the follower's estimated goal energy $\hat{\theta}_E^{\mathrm{d}}$ converges for a step in the reference variable $\theta_E^{\mathrm{d}}(t) = \sigma(t)\theta_E^{\mathrm{d}}$ to the right value as $t \to \infty$, because $\lim_{s \to 0} G_{\vartheta_r \to \hat{\theta}_E^{\mathrm{d}}}^{\mathrm{ge}} G^{\mathrm{ge}} = 1$.

V. ADAPTIVE ENERGY CONTROL FOR THE T-PENDULUM

In this section we apply the fundamental dynamics based adaptive energy control of Sec. IV to a complex pendulum as the t-pendulum. Figure 3 shows the block diagram for the follower control structure for the t-pendulum simulation. The leader control structure is similar to the one of the goal estimation follower (yellow background), but with external reference variable θ_E^{d} instead of the internal estimation of $\hat{\theta}_E^{\mathrm{d}}$. In the following, details are given on the projection onto the abstract simple pendulum and the complete control law formulation from the perspective of the follower agent $\mathcal{F}$. The same applies for the leader agent $\mathcal{L}$.

A. Projection onto the abstract simple pendulum

As defined in the problem statement in (1) and (2), the agents are limited to force feedback $\boldsymbol{F}_{\mathcal{F}}$. From the measured interaction forces $\boldsymbol{F}_{\mathcal{F}}$ a first approximation of the projected deflection angle ϑ in Fig. 1 is computed by

$$\vartheta_F = \arctan\left(\frac{-F_{\mathrm{p},\mathcal{F},x}}{F_{\mathrm{p},\mathcal{F},y}}\right), \tag{27}$$

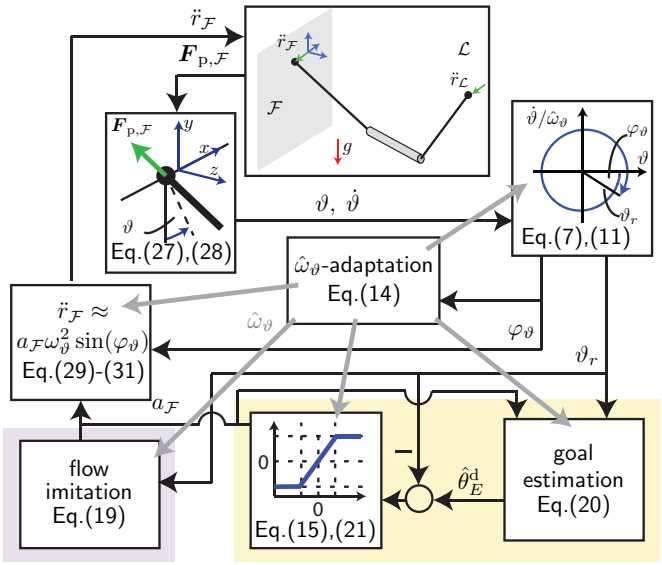

Fig. 3. Block diagram of the follower control structure for the t-pendulum simulations. The goal estimation branch (yellow background) and the flow imitation branch (purple background) represent the two follower alternatives for the computation of the amplitude factor $a_\mathcal{F}$.

where $\boldsymbol{F}_{\mathrm{p},\mathcal{F}} = \begin{bmatrix} F_{\mathrm{p},\mathcal{F},x} & F_{\mathrm{p},\mathcal{F},y} & F_{\mathrm{p},\mathcal{F},z} \end{bmatrix}^T$ is the resultant force that acts onto the pendulum and is obtained through dynamic compensation of the handle induced forces by $\boldsymbol{F}_{\mathrm{p},\mathcal{F}} = \boldsymbol{F}_\mathcal{F} - m_{\mathrm{h},\mathcal{F}} \begin{bmatrix} \ddot{r}_\mathcal{F} & -g & 0 \end{bmatrix}^T$.

We obtain the complete cartesian state with equal phase shift through filtering

$$\dot{\vartheta} = G_{\mathrm{hp}}(T_\vartheta)\vartheta_F, \quad \vartheta = G_{\mathrm{lp}}(T_\vartheta)\vartheta_F, \tag{28}$$

where G_{hp} and G_{lp} are first-order high- and low-pass filters with time constant T_ϑ.

1) Complete control law: In order to obey a restricted workspace and to filter out remaining high frequency oscillations on the phase angle φ_ϑ (see Fig. 2) as well as noise, Yoshida [7] suggests to construct a reference trajectory

$$r_\mathcal{F}^{\mathrm{d}} = -\frac{a_\mathcal{F}}{|G(j\hat{\omega}_\vartheta)|}\sin(\varphi_\vartheta - \angle G(j\hat{\omega}_\vartheta)), \tag{29}$$

which is filtered by the second-order filter

$$G(s) = \frac{\ddot{r}}{r^{\mathrm{d}}} = \frac{s^2\left(\frac{\hat{\omega}_\vartheta}{c_0}\right)^2}{s^2 + 2\zeta\frac{\hat{\omega}_\vartheta}{c_0}s + \left(\frac{\hat{\omega}_\vartheta}{c_0}\right)^2}, \tag{30}$$

where c_0 and ζ are design parameters. The commanded acceleration results in

$$\ddot{r}_\mathcal{F} \simeq a_\mathcal{F}\,{\omega_\vartheta}^2\frac{|G(j\omega_\vartheta)|}{|G(j\hat{\omega}_\vartheta)|}\sin(\varphi_\vartheta - \angle G(j\hat{\omega}_\vartheta) + \angle G(j\omega_\vartheta)) \approx a_\mathcal{F}\,{\omega_\vartheta}^2\sin(\varphi_\vartheta). \tag{31}$$

Consequently, the reference trajectory is designed such that it compensates for the amplitude shift $|G(j\omega_\vartheta)|$ and phase shift $\angle G(j\omega_\vartheta)$ produced by the filter at the natural frequency ω_ϑ of the pendulum for $\hat{\omega}_\vartheta \approx \omega_\vartheta$. Note that according to (29), (15) and (19) the maximum amplitude factor $\bar{a}$ serves as a workspace restriction for the agents.

VI. SIMULATION EXPERIMENT

The controller was evaluated in simulation based on the fundamental dynamics and with a multi body simulation of the t-pendulum. In this section we first report on the fundamental dynamics simulation results, which show how the different follower controllers perform in an idealized scenario. This is followed by the t-pendulum simulations, in which we analyze how the controllers behave in interaction with a realistic complex pendulum-like object.

A. Main results of fundamental dynamics simulations

The fundamental dynamics simulations confirmed the theoretically obtained properties of Sec. IV-C. Further important results are given below.

1) Follow-up behavior: Both follower approaches achieved perfect follow up behavior $\vartheta_r \to \theta_{E\mathrm{m}}$ for $T_f \to 0$.

2) Stability bounds: The flow imitation approach had an higher absolute stability margin with respect to estimation errors $\hat{B}_\mathcal{F} < B$ than the goal estimation approach.

3) Effort sharing: For zero estimation errors, the goal estimation follower achieved any desired relative follower contribution $\gamma_\mathcal{F}^{\mathrm{d}} \in]0,1[$ without overshoot. In contrast, for increasing $\gamma_\mathcal{F}^{\mathrm{d}}$ the flow imitation approach led to an increasing overshoot of the energy ϑ_r with respect to the goal energy θ_E^{d} for $\gamma_\mathcal{F}^{\mathrm{d}} > 1 - \gamma_\mathcal{L}^{\mathrm{d}}$ and a slower transfer behavior for $\gamma_\mathcal{F}^{\mathrm{d}} = 1 - \gamma_\mathcal{L}^{\mathrm{d}}$.

B. T-pendulum simulation setup

We performed the simulations using *MATLAB/Simulink*. The t-pendulum was modeled through rigid bodies that are connected via spherical joints using the 1st generation *SimMechanics* toolbox (see [3] for implementation details and the t-pendulum parameters). The control parameters were $T_\omega = 2\,\mathrm{s}$, $T_f = 1\,\mathrm{s}$, $T_\vartheta = 0.1\,\mathrm{s}$, $K_{\mathrm{d}} = \hat{K}_{\mathrm{d}} = 0.4\,{}^1\!/_{\mathrm{s}}$, $\bar{a} = 0.5\,\mathrm{m}$, $c_0 = 0.9$ and $\zeta = 1.2$.

C. Measures for the t-pendulum simulations

1) Analysis of controller performance: The controller performance was based on the settling time T_{s}, the steady state error e and the overshoot o. We defined the settling time T_s to be the time after which the energy of the θ-oscillation stays within a $2\,\%$ band around the steady state energy $\bar{\theta}_E$. The steady state error captured the difference between desired and steady state energy $e = \theta_E^{\mathrm{d}} - \bar{\theta}_E$ and the overshoot was equal to the maximum difference between actual and steady state energy $o = \max_t(\theta_E(t) - \bar{\theta}_E)$.

2) Analysis of effort sharing: The computation of the relative follower contribution as defined in (2) requires computation of the energy flows $\dot{\theta}_{E,\mathcal{L}/\mathcal{F}}$ for which we would need to rely on the abstract simple pendulum approximation. Instead, we computed the relative follower contribution as

$$\hat{\gamma}_\mathcal{F} = \frac{\int_0^{T_{\mathrm{s}}} \dot{E}_\mathcal{F}\,\mathrm{d}\tau}{\int_0^{T_{\mathrm{s}}} \dot{E}_\mathcal{F} + \dot{E}_\mathcal{L}\,\mathrm{d}\tau}, \tag{32}$$

based on the complete energy flows $\dot{E}_{\mathcal{L}/\mathcal{F}} = \dot{\boldsymbol{r}}_{\mathcal{L}/\mathcal{F}}^T \boldsymbol{F}_{\mathrm{p},\mathcal{L}/\mathcal{F}}$.

D. Results and discussion for the t-pendulum simulations

Our control approach cannot start from the lower stable equilibrium $\theta = \dot{\theta} = \psi = \dot{\psi} = 0$, because it requires a rising phase angle φ_ϑ. In reality, this problem can be circumvented by a short jerky motion by the leader. For the simulations we initialized the t-pendulum with small initial angles $\theta(t = 0) = -2.6\,\mathrm{deg}$ and $\psi(t = 0) = -3.0\,\mathrm{deg}$. The $\hat{\omega}_\vartheta$-adaptation was initialized for the leader and the follower with $\hat{\omega}_\vartheta(t = 0) = 6\,\mathrm{rad/s}$. Note that these initial conditions were challenging for our control approach, because the undesired oscillation was initially more dominant than the desired oscillation and the $\hat{\omega}_\vartheta$-adaptation started in between the frequencies of the two oscillations $\omega_\theta \approx 4\,\mathrm{rad/s}$ and $\omega_\psi \approx 8\,\mathrm{rad/s}$. However, the initialization with $\hat{\omega}_\vartheta(t = 0) = 6\,\mathrm{rad/s} > \omega_\theta$ does reflect the guideline $\hat{B}_\mathcal{F} > B$ that originated from the stability analysis in Sec. IV-C. Another difficulty was posed by commanding desired relative contributions $\gamma^\mathrm{d}_\mathcal{F} = 0.6 > \gamma^\mathrm{d}_\mathcal{L} = 0.4$. The goal energy was set to $\theta^\mathrm{d}_E = 45\,\mathrm{deg}$.

The results for the flow imitation approach are given in the upper part of Fig. 4(1a-c) and for the goal estimation approach in the middle part of Fig. 4(2a-c). The bottom part of Fig. 4(3a-c) shows additional results for the goal estimation approach based on second-order filters instead of the first-order filters for the goal energy estimation (see Sec. IV-B).

1) Follow-up behavior: For all presented results, the energy θ_E increased with a clear delay with respect to the reference dynamics $\theta_{E\mathrm{m}}$. Almost perfect reference dynamics tracking was achieved for two leaders or the flow imitation as well as the original goal estimation approach, if $\hat{\omega}_\vartheta$ was set to ω_θ, the t-pendulum was initialized with $\psi(t = 0) = 0$, the time constant[5] $T^\mathrm{fi}_f = 0.1\,\mathrm{s}$ was used and the exact angles θ and $\dot{\theta}$ were made available. Note that the agents' amplitude factors never saturated, as $r_\mathrm{max} = 0.05\,\mathrm{m}$.

2) Performance: The flow imitation approach settled after an overshoot of $o^\mathrm{fi} = 2.8\,\mathrm{deg}$ close to the goal energy θ^d_E at time $T^\mathrm{fi}_\mathrm{s} = 19\,\mathrm{s}$ and under a steady state error of $e^\mathrm{fi} = -2.0\,\mathrm{deg}$. The ψ-oscillation had a maximum energy of $\psi^\mathrm{fi}_{E,\mathrm{max}} = 4.4\,\mathrm{deg}$ and settled at around $\psi^\mathrm{fi}_{E,\mathrm{s}} = 2.9\,\mathrm{deg}$.

The goal estimation approach without additional filter did not settle within 2 % of its steady state value $\bar{\theta}_E$. The average steady state error was $e^\mathrm{ge} = 0.3\,\mathrm{deg}$ and the highest overshoot $o^\mathrm{ge} = 4.2\,\mathrm{deg}$ occurred at $t = 11\,\mathrm{s}$. The reason for this unsatisfactory performance was the sensitivity of the goal estimation with respect to the ψ-oscillation. The ψ-oscillation caused the goal energy estimate $\hat{\theta}^\mathrm{d}_E$ to oscillate, which in turn excited the ψ-oscillations. At $t = 25\,\mathrm{s}$ the undesired ψ oscillation contained an energy of $\psi_E = 19\,\mathrm{deg}$.

The bottom part of Fig. 4(3a-c) shows that additional low-pass filtering of the goal energy estimate increased the performance. The energy θ_E settled after a negligible overshoot of $o^\mathrm{ge,o2} = 0.2\,\mathrm{deg}$ at $T^\mathrm{ge,o2}_\mathrm{s} = 13\,\mathrm{s}$ with a steady state error $e^\mathrm{ge,o2} = -2.7\,\mathrm{deg}$. The ψ-oscillation contained a maximum energy of $\psi^\mathrm{ge,o2}_{E,\mathrm{max}} = 4.1\,\mathrm{deg}$ and settled at only $\psi^\mathrm{ge,o2}_{E,\mathrm{s}} = 0.8\,\mathrm{deg}$.

[5]for the original goal estimation approach increasing oscillations were observed for $T^\mathrm{ge}_f = 0.1\,\mathrm{s}$.

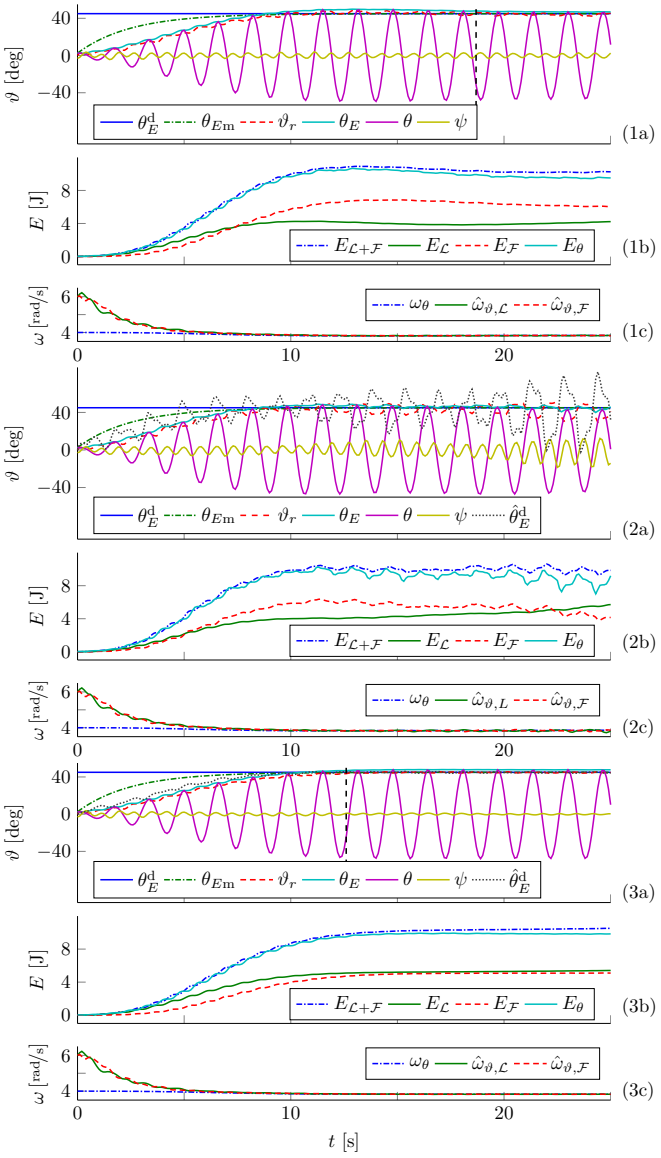

Fig. 4. Flow imitation (1a-c), goal estimation (2a-c), goal estimation with second order filtering (3a-c): a) Angles θ and ψ, goal energy θ^d_E, reference dynamics $\theta_{E\mathrm{m}}$, energy equivalents θ_E and from leader perspective ϑ_r, b) energy contained in the θ-oscillation E_θ, energies injected by the agents $E_\mathcal{L}$ and $E_\mathcal{F}$ and their sum $E_{\mathcal{L}+\mathcal{F}}$, c) natural frequency ω_θ and its leader and follower estimates $\hat{\omega}_{\vartheta,\mathcal{L}}$ and $\hat{\omega}_{\vartheta,\mathcal{F}}$.

3) Effort sharing: The slightly increasing difference between the energies $E_{\mathcal{L}+\mathcal{F}}$ and E_θ in Fig.4(1b) and (3b) is due to minimal damping. In contrast, the increasing difference in Fig.4(2b) stems from the excitation of the ψ-oscillation. The flow imitation approach almost perfectly achieved the desired relative follower contribution $\gamma^\mathrm{fi}_\mathcal{F} = 0.63 \approx \gamma^\mathrm{d}_\mathcal{F}$. The original goal estimation achieved $\gamma^\mathrm{ge}_\mathcal{F} = 0.57 \approx \gamma^\mathrm{d}_\mathcal{F}$ if we set the settling time to $T^\mathrm{ge}_\mathrm{s} = 15\,\mathrm{s}$. In contrast, the goal estimation with second-order filters only reached $\gamma^\mathrm{ge,o2}_\mathcal{F} = 0.48$. This is due to the choice of k_γ based on the first-order filters. Computation of the transfer functions in Sec. IV-C for

the second-order filters with time constant T_f and damping D_f yields

$$k_\gamma^{2\mathrm{o}} = \frac{1}{1 - 2T_f D_f \hat{K}_\mathrm{d}}. \tag{33}$$

Consequently, for our choice of reference dynamics with $\hat{K}_\mathrm{d} = K_\mathrm{d} = 0.4$ and a time constant of $T_f = 1$, we already obtain a high gain $k_\gamma^{2\mathrm{o}} = 5$ and are close to the stability borders with a damping of $D_f = 1$. Lower damping values led to increased oscillations of θ_E and $\hat{\theta}_E^\mathrm{d}$, even for the fundamental dynamics simulations. Therefore, we refrained from enforcing the relative follower contribution and used k_γ from (25) for an improved transient behavior and a greater absolute stability margin. In contrast, the flow imitation approach was able to achieve $\gamma_\mathcal{F} = 0.85$ for $\gamma_\mathcal{F}^\mathrm{d} = 0.9$.

4) Fundamental dynamics approximation: Figures 4(1a) and (3a) show that for low ψ-oscillation, the state space radius ϑ_r closely tracked the energy θ_E. Furthermore, the $\hat{\omega}_\vartheta$-adaptation approached the actual natural frequency ω_θ for all simulations. The close tracking as well as the successful $\hat{\omega}_\vartheta$-adaptation support the applicability of the fundamental dynamics approximation to a complex pendulum-like object as the t-pendulum. With increased undesired ψ-oscillation the projection of the t-pendulum behaved less as the abstract simple pendulum. This became visible in the increased oscillations of ϑ_r and $\hat{\omega}_\vartheta$ (see Fig. 4(2a) and (2c)).

In summary, the control goals as stated in (1) and (2) were differently well achieved for the two leader-follower structures. Both leader-follower structures led to a significantly delayed swing-up with respect to the desired reference dynamics and consequently a high ϵ_θ. Whereas the goal estimation with additional filtering achieved faster settling and lower bounds on ϵ_ψ, the flow imitation approach allowed for higher desired relative energy contribution for the follower $\gamma_\mathcal{F}^\mathrm{d}$ with tighter bounds $\epsilon_\mathcal{F}$.

VII. CONCLUSIONS

This paper proposes an adaptive energy controller for cooperative swinging of complex pendulum-like objects by two agents. The fact that the desired oscillation of the complex pendulum-like object under consideration can be approximated by a simple pendulum oscillation, allows us to apply the fundamental dynamics of a simple pendulum to the two-agent system. The linear fundamental dynamics enable the design of two adaptive leader-follower control structures. An analysis of the adaptive control structures yields analytical results for properties as stability, stationary transfer behavior and resultant relative energy contribution of the agents under the fundamental dynamics assumption. Simulation experiments with a complex pendulum-like object show the applicability of the adaptive control structures to a highly nonlinear two-agent pendulum. The undesired oscillation does affect the validity of the fundamental dynamics approximation. However, the simulations show that the undesired oscillation is kept within small bounds for both adaptive leader-follower control structures.

In future work, we plan to analyze the influence of the undesired oscillation more thoroughly, in order to answer questions as under which circumstances the undesired oscillation instead of the desired oscillation is excited. Furthermore, we want to test the proposed control approaches in a realistic setup, with noisy force data and variable behavior of the other agent. Also, we are interested in extending our approach towards swinging of more realistic flexible objects that enforce a stronger coupling between the agents.

ACKNOWLEDGMENT

The authors would like to thank Stefan Kersting for his valuable feedback.

REFERENCES

[1] M. T. Mason and K. Lynch, "Dynamic manipulation," in *Proc. IEEE/RSJ IROS*, vol. 1, Jul 1993, pp. 152–159 vol.1.

[2] P. Donner, A. Mörtl, S. Hirche, and M. Buss, "Human-robot cooperative object swinging," in *Proc. IEEE ICRA*, May 2013, pp. 4343–4349.

[3] P. Donner, F. Christange, and M. Buss, "Human-robot cooperative swinging of complex pendulum-like objects," in *Proc. IEEE/RSJ IROS*, Nov 2013, pp. 4602–4608.

[4] C. de Crousaz, F. Farshidian, and J. Buchli, "Aggressive optimal control for agile flight with a slung load," in *IEEE/RSJ IROS Workshop on Machine Learning in Planning and Control of Robot Motion*, 2014.

[5] K. Åström and K. Furuta, "Swinging up a pendulum by energy control," *Automatica*, vol. 36, no. 2, pp. 287 – 295, 2000.

[6] R. Lozano, I. Fantoni, and D. Block, "Stabilization of the inverted pendulum around its homoclinic orbit," *Systems and Control Letters*, vol. 40, no. 3, pp. 197–204, 2000.

[7] K. Yoshida, "Swing-up control of an inverted pendulum by energy-based methods," in *Proc. ACC*, vol. 6, 1999, pp. 4045–4047.

[8] M. Bernard and K. Kondak, "Generic slung load transportation system using small size helicopters," in *Proc. IEEE ICRA*, 2009, pp. 3258–3264.

[9] D. Zameroski, G. Starr, J. Wood, and R. Lumia, "Rapid swing-free transport of nonlinear payloads using dynamic programming," *Journal of Dynamic Systems, Measurement, and Control*, vol. 130, no. 4, p. 041001, 2008.

[10] N. Zoso and C. Gosselin, "Point-to-point motion planning of a parallel 3-dof underactuated cable-suspended robot," in *Proc. IEEE ICRA*, May 2012, pp. 2325–2330.

[11] Y. Maeda, A. Takahashi, T. Hara, and T. Arai, "Human-robot cooperation with mechanical interaction based on rhythm entrainment-realization of cooperative rope turning," in *Proc. IEEE ICRA*, vol. 4, 2001, pp. 3477–3482 vol.4.

[12] C. H. Kim, K. Yonekura, H. Tsujino, and S. Sugano, "Physical control of the rotation center of an unsupported object rope turning by a humanoid robot," in *Proc. IEEE-RAS Humanoids*, Dec 2009, pp. 148–153.

[13] C. G. Atkeson and S. Schaal, "Robot learning from demonstration," in *ICML*, vol. 97, 1997, pp. 12–20.

[14] K. Doya, "Reinforcement learning in continuous time and space," *Neural computation*, vol. 12, no. 1, pp. 219–245, 2000.

[15] I. Palunko, P. Donner, M. Buss, and S. Hirche, "Cooperative suspended object manipulation using reinforcement learning and energy-based control," in *Proc. IEEE/RSJ IROS*, Sept 2014, pp. 885–891.

[16] E. Najafi, G. Lopes, and R. Babuska, "Reinforcement learning for sequential composition control," in *Proc. IEEE CDC*, Dec 2013, pp. 7265–7270.

[17] P. Donner, F. Christange, and M. Buss, "Adaptive simple pendulum swing-up controller based on the closed-loop fundamental dynamics," in *Proc. ECC*, 2015.

[18] C. G. Carvalhaes and P. Suppes, "Approximations for the period of the simple pendulum based on the arithmetic-geometric mean," *American Journal of Physics*, vol. 76, no. 12, pp. 1150–1154, 2008.

[19] P. Donner, F. Christange, and M. Buss, "Detailed derivations for the analysis of the fundamental dynamics based leader-follower structures," http://www.shrine-project.eu/?Publications.